ACS OMEGA

Article

http://pubs.acs.org/journal/acsodf

Auxiliary Biomembranes as a Directional Delivery System To Control Biological Events in Cell-Laden Tissue-Engineering Scaffolds

Helena Knopf-Marques,[†,‡,▽] Julien Barthes,[†,§,▽] Lucie Wolfova,[∥] Bérengère Vidal,[§] Geraldine Koenig,[†] Jalal Bacharouche,[⊥] Grégory Francius,[⊥] Helle Sadam,[#] Urmas Liivas,[#] Philippe Lavalle,*[,†,‡] and Nihal Engin Vrana*[,†,§]

[†]INSERM UMR 1121, 11 rue Humann, 67085 Strasbourg, France

[‡]Faculté de Chirurgie Dentaire, Université de Strasbourg, 8 rue Sainte Elisabeth, 67000 Strasbourg, France

[§]PROTiP Medical, 8 Place de l'Hôpital, 67000 Strasbourg, France

[∥]Contipro Biotech S.R.O., Dolni Dobrouc 401, 561 02 Dolni Dobrouc, Czech Republic

[⊥]Laboratoire de Chimie Physique et Microbiologie pour l'Environnement, CNRS, UMR 7564, 405 rue de Vandoeuvre, 54600 Villers-les-Nancy, France

[#]Protobios LLC, 12618 Tallinn, Estonia

Supporting Information

ABSTRACT: Delivery of growth factors is an indispensable part of tissue engineering. Here, we describe a detachable membrane-based release system composed of extracellular matrix components that can be attached to hydrogels to achieve directional release of bioactive molecules. This way, the release of cytokines/growth factors can be started at a desired point of tissue maturation or directly in vivo. As a model, we develop thin films of an interpenetrating network of double-cross-linked gelatin and hyaluronic acid derivatives. The use of the auxiliary release system with vascular endothelial growth factor results in extensive sprouting by encapsulated vascular endothelial cells. The presence of the release system with interleukin-4 results in clustering of encapsulated macrophages with a significant decrease in M1 macrophages (proinflammatory). This system can be used in conjunction with three-dimensional structures as an auxiliary system to control artificial tissue maturation and growth.

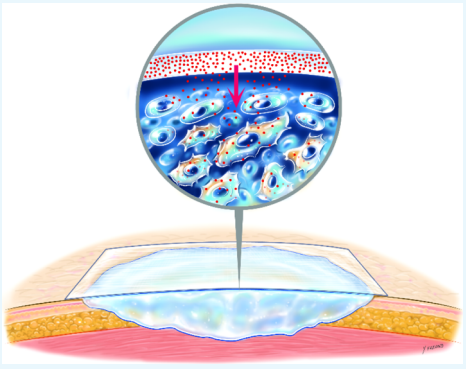

INTRODUCTION

Cells need specific bioactive molecules for adhesion, migration, proliferation, or differentiation. These bioactive molecules are crucial for events such as angiogenesis and osteogenesis or for the modulation of the immune response after implantation.[1] To provide these molecules to the cells, many strategies have been developed using different biomaterials as release platforms.[2] To develop an efficient release platform, two main parameters must be controlled: (i) the degradation rate of the platform to control the temporal release of the molecules and (ii) the chemical or physical interaction between the material and the molecules to control the loading of the molecules. To this purpose, bioactive molecules have been incorporated in biomaterials mainly through either covalent or noncovalent approaches.[3] However, for tissue engineering purposes, the direct incorporation of the growth factors limits the level of control over the timeline of biological events. A decoupling of the cell-containing parts of tissue-engineering scaffolds and their release component can provide a more modular way to control cell behavior both in vitro and in vivo.

To overcome this problem, another approach can be considered with the development of film-based release platforms that are in direct contact with the cell-containing scaffolds such as cell-laden hydrogels. Film-based release systems ensure an efficient presentation of bioactive agents as the film defines the location of the reservoir distinctly, that is, the bioactive agents will not diffuse from the implantation site immediately. In vivo, one of the most important characteristics of extracellular matrix (ECM) molecules is their ability to act as a reservoir for growth factors; ECM can regulate their activation, synthesis, degradation, and their release into the surrounding environment. For example, vascular endothelial growth factor (VEGF) is known to interact with heparin, heparin sulfate, hyaluronan (HA), and fibronectin. Recombinant human bone morphogenetic protein-2 (rhBMP-2) and rhBMP-7 interact with heparin, heparin sulfate, or collagen.[4] Considering these specific interactions, a release platform with the right biomaterial composition can be designed for long-term growth factor release. Over the past few years, biomaterial systems such as ECM-based scaffolds (gelatin, collagen, HA)

Received: December 14, 2016
Accepted: March 2, 2017
Published: March 15, 2017

DOI: 10.1021/acsomega.6b00502
ACS Omega 2017, 2, 918−929

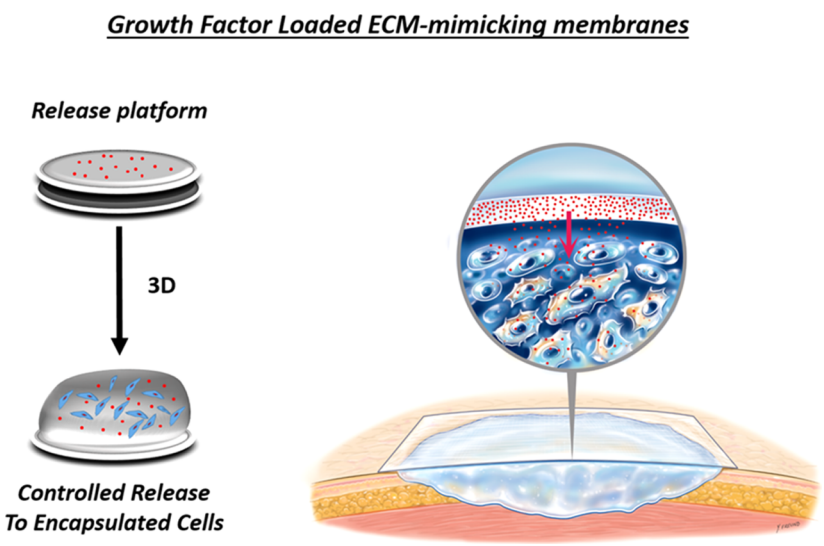

Figure 1. Auxiliary release system for engineered tissues.

and polyelectrolyte multilayer films have been used to load and release bioactive molecules for tissue engineering purposes. Such thin-film-based structures can be produced in a free-standing manner.[5] Recently, our group designed an ECM-mimicking surface coating as an alternative cell culture microenvironment. This ECM-based material is made of thin film of concentrated gelatin made by the spin coating process and enzymatically cross-linked with microbial Ca^{2+}-independent transglutaminase (TGA). This cell feeder platform can provide bioactive molecules, and its stiffness can be modified through the addition of nanoparticles to modulate the cell behavior.[6] However, for more effective retention of growth factors, incorporation of more than one component of ECM would be necessary. In this way, the auxiliary release system, designed in this study, will not only interact with different growth factors in a specific manner but also act as a substrate for incoming cells without inducing adverse immune reactions.

Hyaluronic acid (HA) is a glycosaminoglycan, which plays an important role in cell differentiation, angiogenesis, anti-inflammatory response, and cell growth.[7] Thus, it is a good candidate to design biomaterials if it is combined with other ECM components that promote cell adhesion. To improve mechanical properties of HA and to make a strong gel, it is possible to cross-link HA after chemical modification of its functional groups, for example, by methacrylation or using hydrazide derivatives.[8] Collagen, collagen-like biomaterials such as gelatin, and collagen-/gelatin-based composites have been used for a long time in tissue engineering as drug delivery carriers for bioactive molecules.[9] To mimic natural micro-environment, we have used two ECM components, gelatin type B (denaturated collagen) and HA, to design the release platform.[10] To adjust the physical parameters of the composite gelatin/HA film, tyramine-conjugated HA is used. HA-tyramine (HA-tyr) can be cross-linked by the horseradish-mediated reaction[11] using horseradish peroxidase (HRP), and gelatin is enzymatically cross-linked using TGA.[6] Consequently, the resulting film is double-cross-linked and forms an interpenetrating network, which will improve the stability of the composite and its capacity to retain growth factors and cytokines.

In the integration of the engineered soft tissues, two biological events are of particular import: (i) integration of the delivered scaffold with the host vascularization and (ii) a controlled inflammatory response to the implanted system that is resolved in a time scale similar to that for normal wound healing to facilitate and promote healing/integration. An auxiliary delivery system can establish the contact of the engineered tissue with the host vasculature and immune system. The VEGF and interleukin-4 (IL-4) were used as model molecules to be delivered. VEGF is a potent angiogenic growth factor and IL-4 is an established anti-inflammatory cytokine, which has been shown to induce M2 (remodeling inducing) macrophage phenotype. For quantification of vascular endothelial cell and monocyte/macrophage responses to the delivery system in both two dimensions (2D) and three dimensions (3D), human umbilical cord vascular endothelial cells (HUVECs) and a human monocytic cell line (THP-1) cells were utilized.

In this study, we demonstrated the added value of the incorporation of a separate release platform to the tissue-engineering scaffold using a cell delivery system based on cell-laden gelatin hydrogels, which contain as an auxiliary component a spin-coated composite of gelatin and HA-tyr derivatives for controlled release of cytokines and growth factors to the encapsulated cells (Figure 1). The gelatin/HA-tyr film is used as a reservoir of cytokines to obtain a sustained release. As a proof of concept, we quantified the effect of release of VEGF or IL-4 on vascular endothelial cells or human monocytes, respectively, in a 3D culture environment. In this work, gelatin and gelatin/unmodified HA films will be considered as single cross-linked films (TGA) and those of gelatin/HA-tyr as double-cross-linked films (TGA + HRP).

RESULTS AND DISCUSSION

Naturally derived polymers are attractive for tissue engineering because of being the building blocks of the ECM.[12] They have been widely used in a composite form (such as composites of gelatin with HA,[13] chitosan,[14] and silk[15]). HA presents the ability to act as a binding site for molecules. Hence, one important advantage of gelatin−HA composites is the strength of both materials. The synergistic use of gelatin with other materials enables more precise material degradation and controlled release. As the first component of the final system, we first analyzed the distribution of unmodified HA when spin-

DOI: 10.1021/acsomega.6b00502
ACS Omega 2017, 2, 918−929

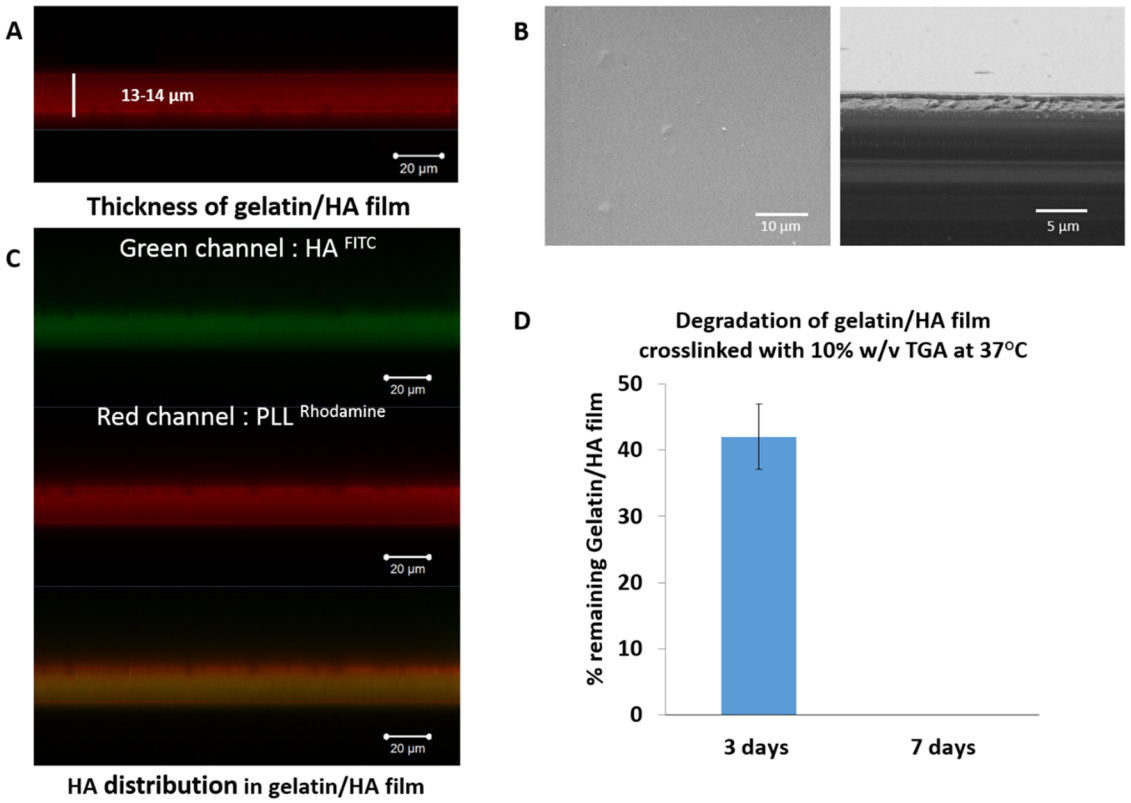

Figure 2. Gelatin/HA film characteristics: (A) Thickness of the film cross-linked with TGA determined by a confocal microscope using PLL^{Rho} as a fluorescent labeling agent. (B) SEM picture of the film (left: *x*,*y* surface, right: cross section). (C) Co-localization of HA^{FITC} and PLL^{Rho} throughout the film thickness determined with a confocal microscope to prove HA homogeneous distribution within the film. (D) Stability of the gelatin/HA film at 37 °C in phosphate-buffered saline (PBS) without poly(ethyleneimine) (PEI) as a first layer after 3 and 7 days.

coated with gelatin and cross-linked with TGA. The composition of this single cross-linked film was 14% w/v gelatin and 1% w/v unmodified HA. Labeled HA was observed to be distributed homogeneously throughout the film thickness (Figure 2C). The average film thickness was estimated to be 13 μm (Figure 2A). Scanning electron microscopy (SEM) analysis of the surface and the cross section of the film demonstrated a smooth, homogeneous surface (Figure 2B). Both gelatin-only and gelatin/unmodified HA films (single cross-linked) were stable in culture conditions up to 3 days; however, the entire film was detached from the surface after 7 days (Figure 2D).

Thus, to ensure a long-term stability of the film, a cross-linkable HA derivative was used to obtain a double-cross-linked composite, an interpenetrating network of gelatin and HA (Figure 3A). To this end, we have used tyraminated HA. Previously, Lee et al. used a H_2O_2/HRP-based cross-linking for encapsulation of mesenchymal stem cells (MSCs), within hydroxyphenylpropionic acid-conjugated gelatin hydrogels. These gels did not have any cytotoxic effect on MSCs and facilitate endothelial differentiation of the encapsulated MSCs.[16] The average thickness of this gelatin/HA-tyr double-cross-linked film was estimated by confocal images to be approximately 15 μm (Figure 3B). When cultured in 2D conditions both with HUVEC and THP-1 cells, all of the films tested lead to the same results in terms of cell viability. The addition of HA-tyr did not have a negative effect on cell viability compared to that of gelatin/HA or gelatin-only films cross-linked with TGA (Figure 3C,D). To improve the stability, an anchoring layer of PEI was deposited on the glass slide before developing films (Figure S1). As it can be seen in Figure S1B, the PEI/gelatin/HA-tyr film presents a better stability until day 7. We have decided to use the gelatin/HA-tyr film for the next part of our study because of the better film stability compared to that of gelatin and gelatin/unmodified HA and the similar cell response in terms of viability.

The mechanical properties of gelatin/unmodified HA and gelatin/HA-tyr films were quantified by the atomic force microscopy (AFM) nanoindentation technique (Figure S3). The double-cross-linked gelatin/HA-tyr film shows an increase of 30% in Young's modulus compared to that in the gelatin/unmodified HA-only film cross-linked with TGA. The addition of HA-tyr without the cross-linking step decreases Young's modulus. This can be attributed to the ability of HA to absorb a large quantity of water, which will decrease the overall stiffness of the material. The gelatin/HA-tyr film presents a lower Young modulus (28 ± 7 kPa) than that from gelatin/unmodified HA (44 ± 4 kPa), although both have been cross-linked only by TGA. However, once the gelatin/HA-tyr film is cross-linked by the action of the enzyme HRP (double-cross-linked film), its Young modulus increases (58 ± 6 kPa). Moreover, one main advantage of the double-cross-linked interpenetrating network structure is the significant improvement in the stability of the films. The double-cross-linked gelatin/HA-tyr film was stable under the culture conditions up to 21 days. In addition, this film can be obtained as a self-standing membrane by depositing a sacrificial layer on top of the glass slide before the spin-coating process. This layer decreases the interaction between the film and the glass slide, and the film is detached easily once immersed in water (Figure S3).

DOI: 10.1021/acsomega.6b00502
ACS Omega 2017, 2, 918−929

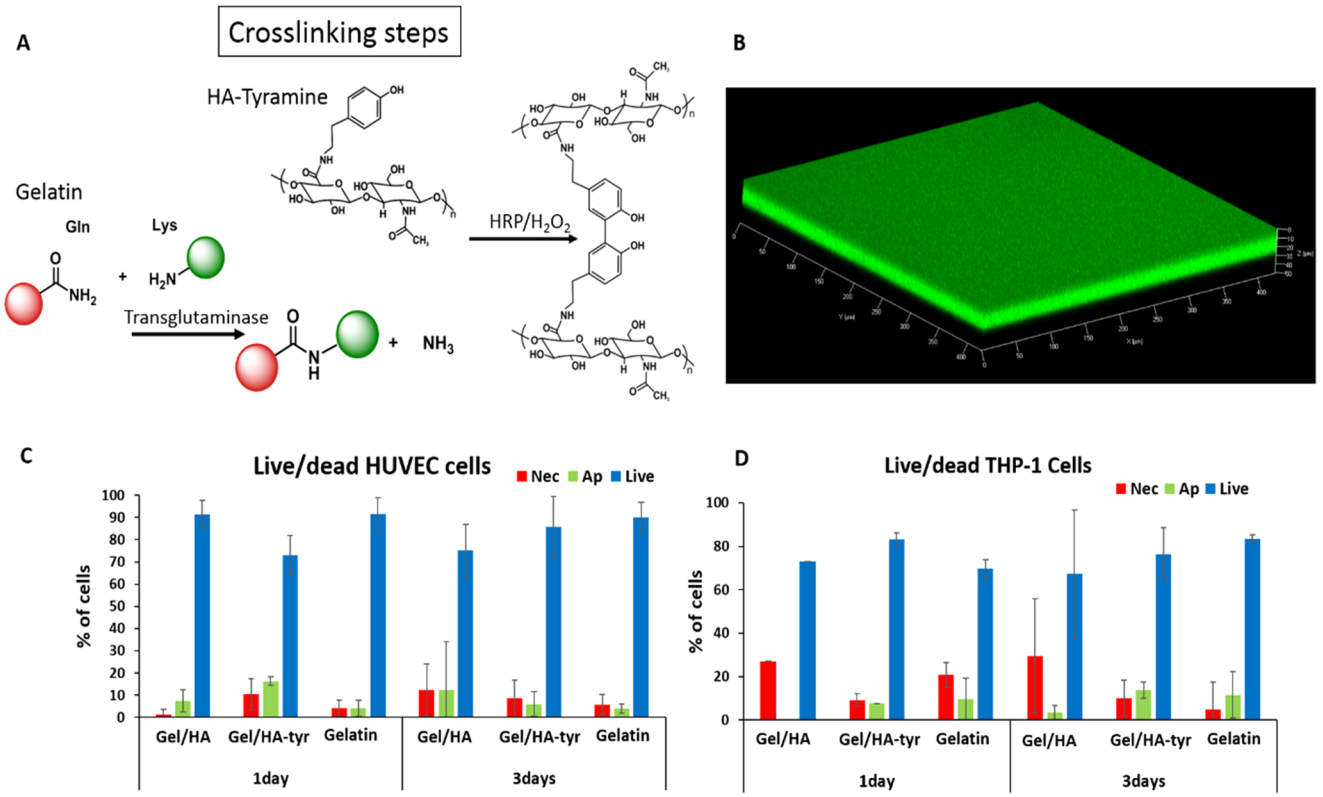

Figure 3. (A) Schematic representation of the strategy to obtain the double-cross-linked gelatin/HA-tyr film. (B) Three-dimensional confocal pictures of the gelatin/HA-tyr film cross-linked with TGA and HRP and fluorescently labeled with BSA^{FITC}. Apoptotic/necrotic/healthy cell quantification for HUVECs (C) and THP-1 cells (D) seeded on gelatin and gelatin/HA derivative (unmodified and tyramine) films for 1 and 3 days. The experiment was performed on three different samples for each condition.

Huang et al. recently showed that a disulfide-cross-linked semi-interpenetrating network of collagen and RGD-functionalized HA can be used for the sustained release of rhBMP-2. On titanium implants, this coating system resulted in increased removal torque compared to that on titanium implants in an in vivo rabbit implantation model. This indicates an improved integration of the coated implant with the surrounding bone tissue. Moreover, they showed that disulfide cross-linking improved the stability of the coating up to 14 days and sustained the release of rhBMP-2 for 10 days.[17] In film format, Crouzier et al. also studied the loading and the long-term release of rhBMP-2 from cross-linked poly(L-lysine)/HA films for controlled differentiation of C2C12 cells to osteoblasts.[18] Using a reservoir/barrier system made of PLL/HA as a reservoir and PAH/PSS as a mechanosensitive barrier, a platform that can release drug with enzymatic degradation triggered by mechanical stimuli has been developed that can be applied to the current system in tissues that are mechanically active.[19] However, one disadvantage of such a system is the limitation of growth factor loading just after the manufacture of the release platform.

In our case, there are two possibilities for the loading of the growth factors, which will lead to different release profiles: (i) the deposition of the desired amount of growth factor onto the preformed films (Figure 4A) and (ii) incorporation of the growth factors during film formation (Figure 4B). To quantify the differences in the released growth factors and their release profiles, VEGF and IL-4 release from the films produced by both methods was monitored by ELISA for 6 days (Figure 4C–F). Even though incorporation of the growth factors into the film production potentially improves the loading, it significantly decreased the amount of bioactive agent available for both IL-4 and VEGF upon release (Figure 4D–F). This may be attributed to the cross-linking of the bioactive molecules inside the film with TGA. When the bioactive molecules are incubated on the preformed film (Figure 4C,E), we can observe a steady release of the growth factors up to 144 h after an initial burst release.

Most of the systems developed for the release of bioactive molecules were based on the encapsulation of the molecules into micro-nanoparticles, and their release was achieved through the degradation of these particles.[20] The main problem with this approach is the difficulty of restricting the particle presence to a specific target, as particularly nanoparticles can diffuse within the host quite easily. There are potential side effects due to the random distribution of the particles inside the host. Direct incorporation of growth factors into the gels without covalent immobilization leads to the rapid leakage of them, which prevents the attainment of the desired effects. Although covalent immobilization can solve the leakage problem, it excludes the possible effect on the incoming cells from the host tissue via release. A dedicated compartment for release in an engineered tissue can both partially solve the leakage problem without affecting the gel properties and enable the interaction with the host tissues via controlled release. To demonstrate that such a directional release is possible, we attached gelatin hydrogels to the film loaded with a fluorescently labeled biomolecule. As a model, we have used fluorescently labeled BSA^{FITC} and labeled the hydrogel with a red fluorescent probe (PLL^{Rho}) to monitor the release of

DOI: 10.1021/acsomega.6b00502
ACS Omega 2017, 2, 918–929

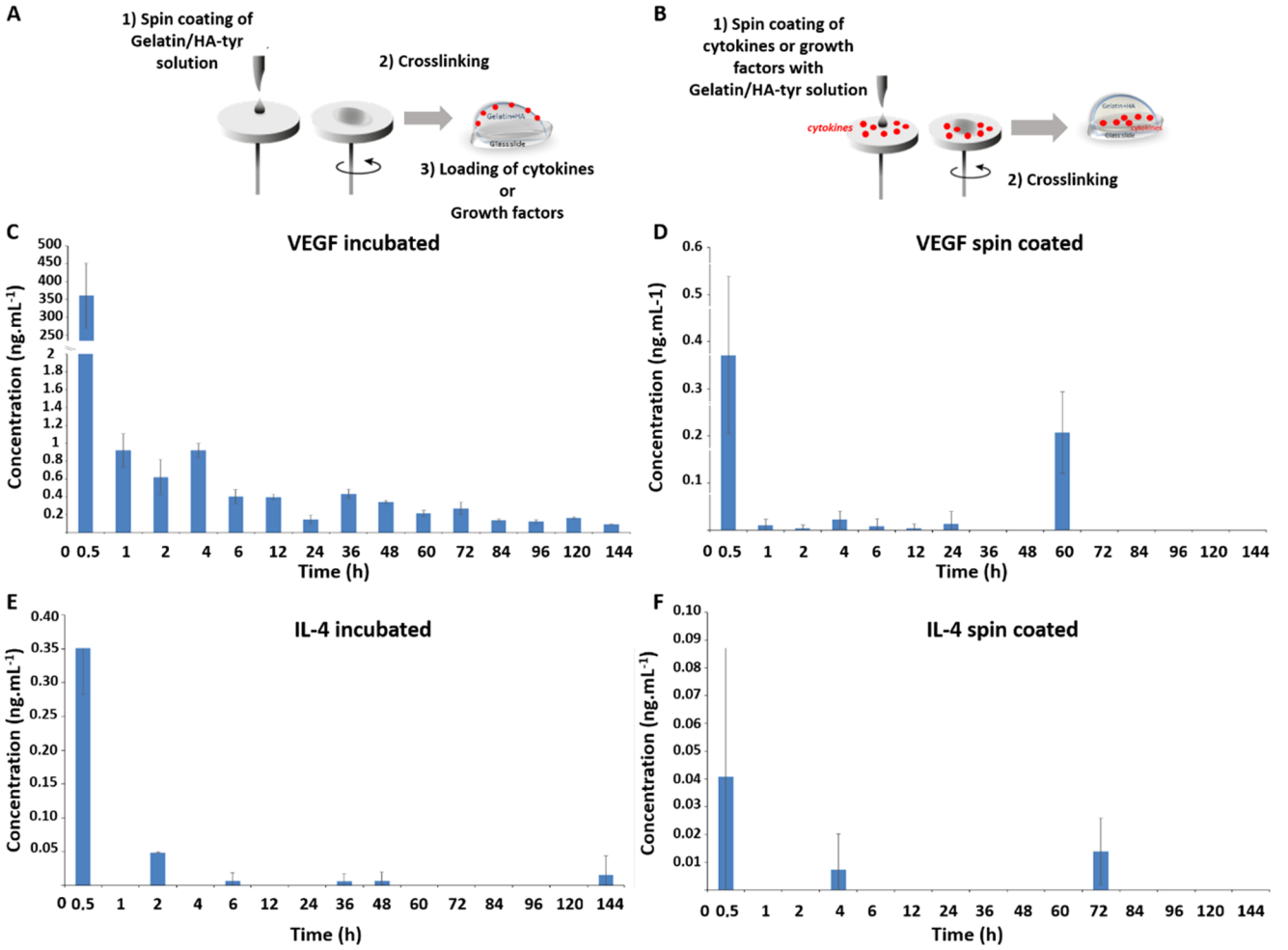

Figure 4. Release of IL-4 and VEGF from gelatin/HA-tyr films. (A, B) Schematic representation of different loading ways of growth factors inside gelatin/HA-tyr cross-linked films. Release profile determined by the ELISA test over 144 h for VEGF (C, D) and IL-4 (E, F) at 37 °C in PBS. For C−F, fresh supernatant was added after each record and three samples for each condition were used.

BSA^{FITC} over time from the film to the hydrogel with a confocal microscope (Figure 5). The hydrogel was labeled with a red fluorescent probe to localize it with a confocal microscope and also to demonstrate the fast release of directly incorporated molecules. In the beginning, the presence of BSA^{FITC} was limited to the film layer, but over time a steady release of BSA^{FITC} into the gel thickness was observed via *xz* sections obtained by confocal microscopy (Figure 5A), and by 144 h, the whole hydrogel thickness contained BSA^{FITC}. More importantly, during this period, the fluorescence in the film layer was maintained, demonstrating the role of reservoir for the film, whereas the loaded rhodaminated PLL slowly diffused out of the structure and the signal was fainter by 144 h. The quantification of the total amount of BSA available in the gel showed a statistically significant increase by 144 h (Figure 5B). The experimental setup is illustrated in Figure 5C.

The effect of IL-4 release was checked for the THP-1 cells directly seeded on the release system. Gelatin/HA-tyr films supported the growth of the THP-1 cells attached on their surface up to 21 days with metabolic activity similar to that of gelatin-only films (Figure 6A). Once, IL-4 was loaded in the films, a decrease in the number of necrotic cells was observed, even though the change is only statistically significant within 90% confidence interval (p = 0.063) (Figure 6B). Moreover, even though high cell numbers were obtained on the films, after 21 days, nearly 80% of the film was still in place, both in the presence and absence of IL-4 (Figure 6C).

To demonstrate the efficacy of the films as a release platform to cells in 3D, our final system is composed of a cell-laden gelatin-based hydrogel cross-linked with TGA fixed to the release system. We have monitored two events under 3D conditions that can be controlled by the presence of growth factors/cytokines: (i) sprouting behavior of vascular endothelial cells and (ii) macrophage phenotype control (specifically differentiation to M2 macrophages). In 3D conditions, for HUVEC cells to form sprouts, the presence of a supporting mesenchyme cell type is generally necessary. In line with this observation, in the absence of VEGF release, HUVECs in the hydrogels have spread in a limited amount with a low degree of organization (Figure 7A), whereas there was significant sprouting in the case of VEGF release by day 14 (Figure 7B). This was accompanied by a significant increase in the metabolic activity of HUVECs under VEGF release conditions, which was maintained up until day 14 (Figure 7C). Nitric oxide is an important biological agent in vascular homeostasis and endothelial cell function, and the low levels of NO secretion by endothelial cells have been implicated with several pathologies including hypertension, heart failure, and diabetes mellitus. HUVECs have secreted up to 25 μM NO (detected as nitrite) in both the absence and the presence of VEGF. The NO levels

DOI: 10.1021/acsomega.6b00502
ACS Omega 2017, 2, 918−929

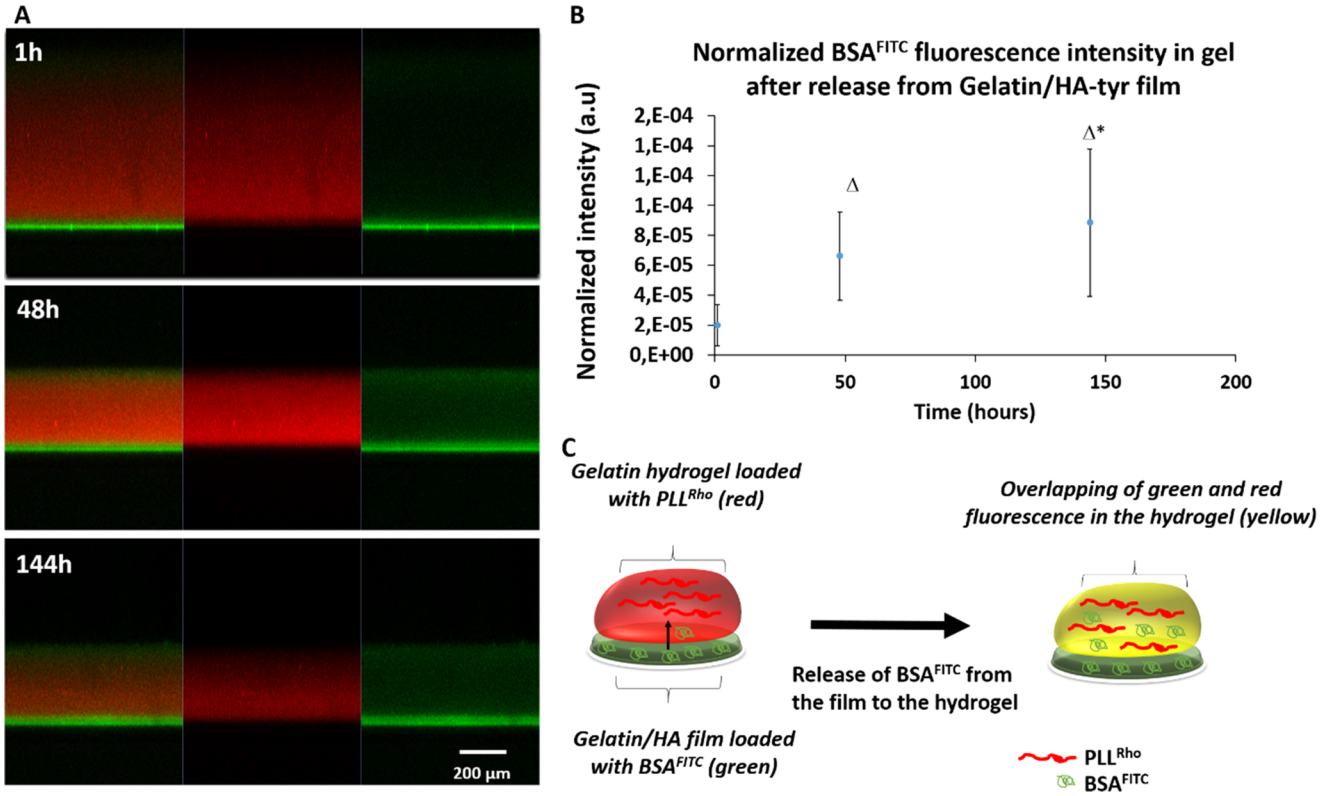

Figure 5. Diffusion of BSA^{FITC} from the film (2D) to the hydrogel (3D). (A) Confocal images of the two-layer system at different time points, with the gelatin/HA-tyr cross-linked film layer labeled with BSA^{FITC} with a 6% w/v gelatin hydrogel cross-linked with a 20% w/v TGA solution labeled with PLL^{Rho} (red fluorescent probe) on top of it. Starting from 1 h, the diffusion of BSA^{FIT} from the film to the hydrogel was monitored (from left to right, the green and red channels are merged, the red channel to localize the hydrogel labeled with the red fluorescent probe and the green channel to localize the film with BSA^{FITC} initially loaded inside). Overtime, we can see the green fluorescence (BSA^{FITC}) initially localized in the film (bottom part) moving to the hydrogel (upper part in red), which means that BSA has diffused from the film to the hydrogel. (B) Quantification of the green fluorescence (BSA^{FITC}) in the hydrogel at different times normalized by the area of the hydrogel ($p \leq 0.05$). (C) Schematic representation of the experimental setup.

increased steadily up until day 10 and then stabilized (Figure 7D).

The availability of the released VEGF in the presence of the cells was quantified after 14 days of culture (Figure S5A). By day 14, still around 500 pg mL^{-1} of VEGF was available. There is a small contribution of the cells' own secretion of VEGF in this, but the amount released under no-VEGF conditions was significantly lower compared to that released under the conditions when VEGF was available. For determining whether the release of VEGF induces the release of other cytokines, we also quantified the levels of several cytokines that are known to be released by endothelial cells (IL-1RA, IL-6, IL-8) by ELISA. There was no detectable release of IL-1RA and IL-6 (Figure S4), but IL-8 was released both in no-VEGF and VEGF release conditions (Figure S5B). By day 10 and day 14, there was significantly higher amount of IL-8 in the medium in the VEGF release conditions in 3D. This is in line with our observations of sprouting in the case of VEGF release, as IL-8 has been demonstrated to be directly involved in the proliferation, survival, and tube formation by endothelial cells and antibody blocking of IL-8 prevents the capillary tube organization.[21] In that condition, cells were cultured in a more proangiogenic microenvironment.

Encapsulation of macrophages in ECM-based hydrogels creates a microenvironment similar to that of tissue macrophages, which are responsible for the homeostasis of the corresponding tissue. In our model, we encapsulated monocytes and, via induction with an M2 phenotype inducing cytokine, we aimed to control the differentiation and phenotype of the encapsulated monocytes. THP-1 cells proliferated in hydrogels up to 21 days either with or without IL-4 release (Figure 8A). However, the cell numbers were significantly higher in IL-4 release samples from day 3 to 14 ($p < 0.05$). The IL-4 release resulted in distinct morphological differences. In IL-4 release samples, THP-1 cells formed large clusters, whereas in no release samples, they were equally distributed within the hydrogel (Figure 8B,C). Clumping during macrophage-like cell differentiation of THP-1 has been stated previously.[22] Moreover, we have observed a distinctly higher CD206 expression by the encapsulated cells with IL-4 compared to that from without IL-4 samples, which is a well-known M2 phenotype marker (Figure 8E,F). Encapsulation itself had a positive effect on the expression of several M2-related genes, such as IL-10, CD163, and IL-1RA compared to THP-1 cells in suspension (Figure S6). However, this increase was accompanied by increase in M1-related genes CD86, STAT-1, IL-6, and TNF-α. Once the IL-4 was released, the expression of M1-related genes significantly decreased (Figure 8D). At protein level, TNF-α release by cells in IL-4 samples was significantly lower compared to that from those in the samples without IL-4 on day 1, after which TNF-α release gradually faded (Figure S7A). The IL-4 release significantly improved the IL-1RA (a M2 marker) secretion by cells (Figure S7B), whereas CCL18 secretion was observed only on day 14

DOI: 10.1021/acsomega.6b00502
ACS Omega 2017, 2, 918−929

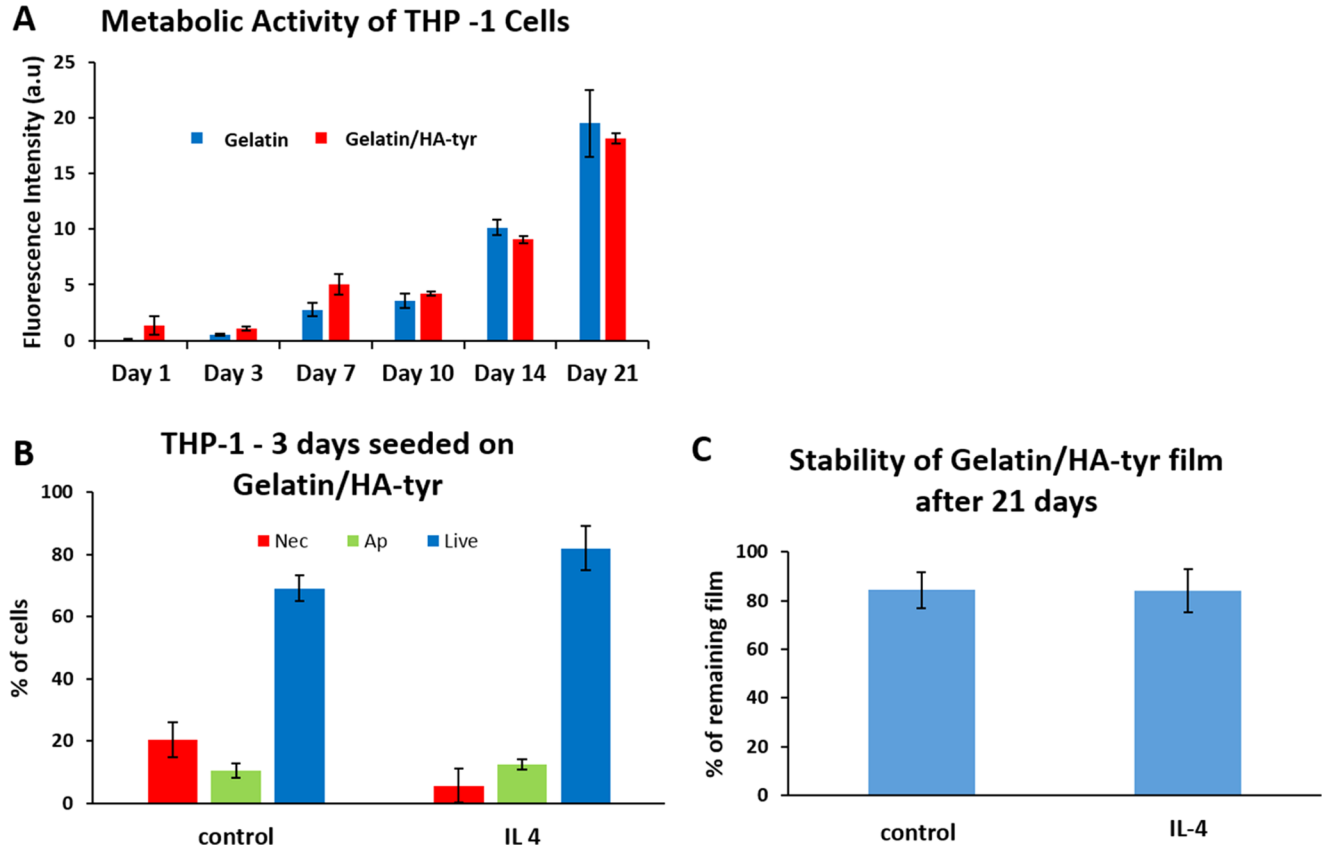

Figure 6. (A) Metabolic activity of THP-1 cells seeded on gelatin and gelatin/HA-tyr films for 21 days. (B) Apoptotic/necrotic/healthy cell quantification for THP-1 cells seeded on gelatin/HA-tyr loaded with IL-4 compared to those on standard gelatin/HA-tyr film (control) after 3 days of culture. (C) The stability of the gelatin/HA-tyr film loaded with IL-4 compared to that of the standard gelatin/HA-tyr film after 21 days in the THP-1 cell culture medium. Each experiment was performed on three different samples.

in both cases (Figure S7C). Overall, the encapsulation of monocytes induced M2 differentiation and the presence of the auxiliary release system augmented the effect.

CONCLUSIONS

Engineering a tissue requires the design of the optimal conditions for the cells in the target tissue involved. Additionally, it is also crucial to develop methods to recruit and direct the host cells that will take an active role in the integration of the implanted tissue. A modular ECM-based biomembrane-controlled release system can be used as a component of engineered tissues for directional release of cytokines and growth factors to attain precise microenvironment control. Development of a system composed of two modular components decouples the release and cell loading, which allows a higher degree of control over the encapsulated cell behavior. We have demonstrated the efficacy of the system for two cell types. Our future work will focus on co-cultures and multifactor release in this configuration.

EXPERIMENTAL SECTION

Material for Gelatin/HA (Gel/HA) Film Construction and Characterization. Gelatin type B (M_w = 2−2.5 × 10^4 Da) from bovine skin, gelatin type A (M_w = 5−10 × 10^4 Da) from porcine skin, fluorescein isothiocyanate-labeled bovine albumin (BSA^{FITC}, M_w = 6.6 × 10^4 Da), and cellulose acetate (M_w = 3 × 10^4 Da) were purchased from Sigma-Aldrich (St. Quentin Fallavier, France). Microbial TGA (M_w = 3.8 × 10^4 Da) was kindly provided by Ajinomoto (Japan). HA (M_w = 3 × 10^5 Da) and HA-tyr (M_w = 3.1 × 10^5 Da) were produced and characterized by Contipro (Dolni Dobrouc, Czech Republic). Human recombinant $VEGF_{165}$ (M_w = 3.82 × 10^4 Da) and human IL-4 (M_w = 1.5 × 10^4 Da) were purchased from Promocell (Germany).

Fluorescein isothiocyanate-labeled poly(L-lysine) (PLL^{FITC}) was obtained from Sigma-Aldrich (St. Quentin Fallavier, France). PLL^{Rho} was synthesized in our laboratory by coupling PLL to rhodamine Red-X, succinimidyl ester (Invitrogen, France).

Spin-Coating of Gelatin/HA Films. Gelatin/HA and gelatin/HA-tyr films were prepared with the solution of gelatin (14% w/v) mixed with HA or HA-tyr (1% w/v) in 0.15 M NaCl/10 mM Tris solutions (pH = 7.4). The gelatin solution (200 μL) at 50 °C was spin-coated (WS-650 Mz-23NPP - Laurell) on a glass slide (diameter of 12 mm) with the following program parameters: rotation speed = 2500 rpm, acceleration = 1250 rpm, and spin-coating time = 2 min. Then, the films were kept dry at 4 °C.

The gelatin film can also be obtained as a self-standing membrane by depositing 60 μL of cellulose acetate (1% w/v in acetone) on top of the glass slide prior to the spin-coating process. Then, after spin-coating, the interactions between cellulose acetate and the glass slide are so weak that the film is detached instantaneously once immersed in water (Figure S4).

Cross-Linking of Gelatin and Gelatin/HA Films. The TGA solution (100 μL, 10%) was incubated on gelatin and gelatin/HA films for 30 min. An additional cross-linking step

DOI: 10.1021/acsomega.6b00502
ACS Omega 2017, 2, 918−929

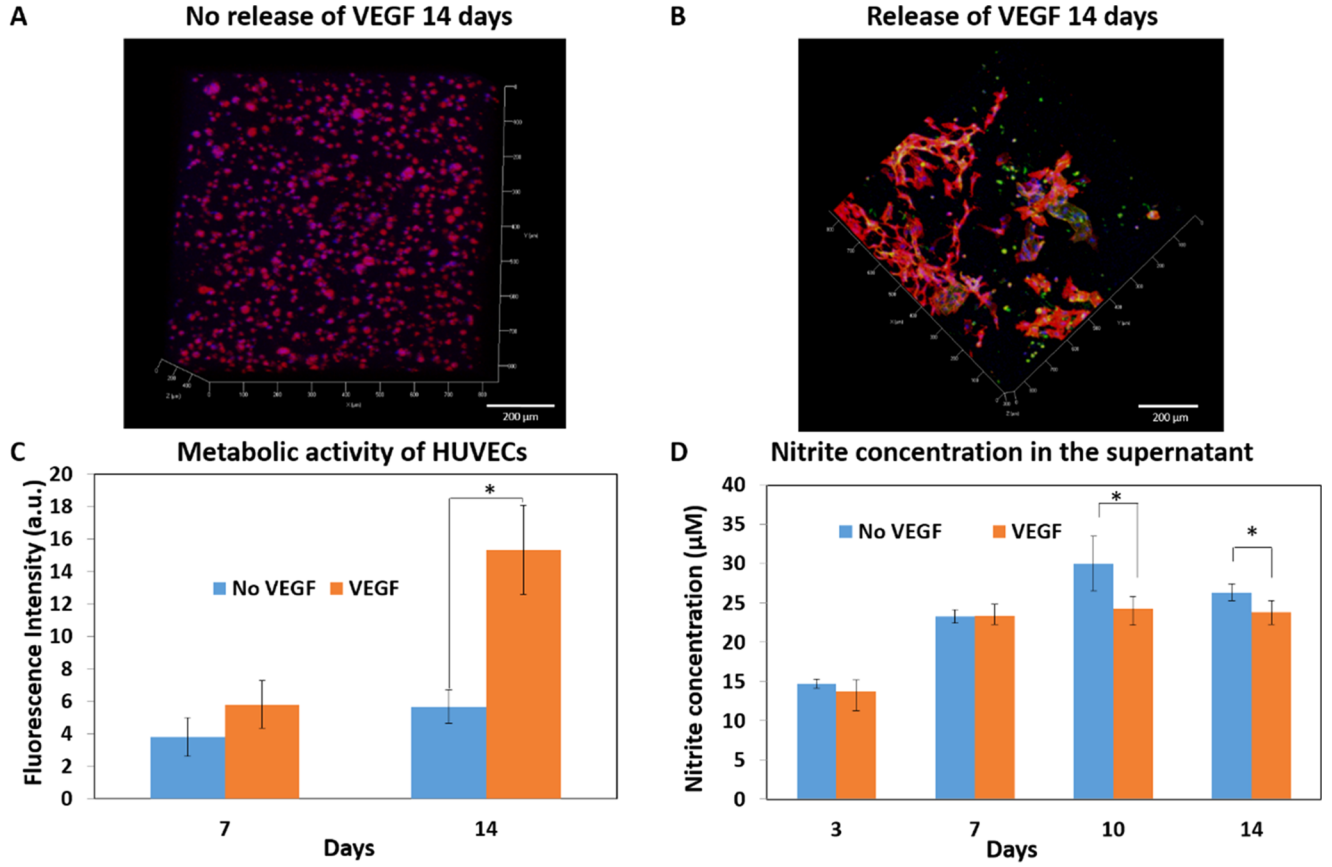

Figure 7. Release of VEGF initially loaded in the gelatin/HA-tyr film to the hydrogel with HUVECs encapsulated. (A, B) Confocal images with DAPI (blue)/phalloidin (red) and PECAM-1 (green) staining after 14 days of experiment with and without VEGF release. (C) Metabolic activity of encapsulated HUVECs in gelatin hydrogels with and without VEGF release from the film (three different samples; $p \leq 0.05$). (D) Nitride oxide quantification via the nitrite detection kit in the supernatant until day 14 of the cell experiment (three different samples; $p \leq 0.05$).

was performed for gelatin/HA-tyr; 100 μL of the H_2O_2/HRP (10:1; 0.24 mg mL^{-1} of HRP in PBS and 0.1 M H_2O_2) solution was incubated on the films for 30 min. After each step, the films were rinsed twice with PBS.

Hydrogel/Film Composite Preparation. A 6% w/v solution of gelatin type A was prepared in MilliQ water at 37 °C. Then, 10 μL of a 20% w/v TGA solution prepared in PBS was added on the cross-linked gelatin/HA-tyr film. The gelatin solution (50 μL) was then deposited on top of the film and mixed with the TGA solution to obtain homogeneous cross-linking, and the system was then put into the incubator at 37 °C for at least 15 min.

SEM and Confocal Laser Scanning Microscopy (CLSM) Analysis. SEM micrograph images were taken on an XL SIRION FEG (FEI Company Eindhoven). CLSM observations were carried out with a Zeiss LSM 710 microscope. To visualize the film and estimate the thickness, the PLL^{Rho} solution was used as a fluorescence probe. Virtual vertical sections can be visualized, hence allowing the determination of the thickness of the film. To check HA distribution within the film, HA^{FITC} was used. HA^{FITC} (0.1% w/v) was mixed with nonlabeled HA (0.9% w/v) and gelatin (14% w/v). Then, PLL^{Rho} was incubated to visualize the film and see if the green and red fluorescence were co-localized, resulting in homogeneous HA distribution.

The diffusion of BSA^{FITC} from the film to the hydrogel was analyzed by confocal microscopy. The gelatin/HA-tyr cross-linked film was labeled in green with BSA^{FITC}. Then, a gelatin hydrogel labeled in red with the PLL^{Rho} solution was added and deposited on top of the film (cf. "Hydrogel/Film Composite Preparation" section) and the system was put into the PBS solution protected from light at 37 °C. Confocal images were taken after few hours at the beginning and then every day to see the diffusion of BSA^{FITC} from the film to the hydrogel. An overlapping between the green and red fluorescence (yellow) can be seen after few hours, which means that BSA diffuses from the film to the hydrogel. Then, using the software incorporated in the machine, we quantified the green fluorescence in the hydrogel and normalized it with the area of the hydrogel to obtain the diffusion profile of BSA^{FITC}.

Degradation Test of Gelatin and Gelatin/HA Films. Degradation tests of gelatin and gelatin/HA films were performed at 37 °C for 3 days by putting films in PBS (2 mL). These films were analyzed using the "Sirius Red/Fast Green Collagen Staining Kit" provided by Chondrex to determine the amounts of collagen and noncollagenous proteins in the sample. The protocol was carried out as described in the kit. These results were compared with those obtained with nondegraded dry gelatin or gelatin/HA films.

Loading of VEGF and IL-4 in Gelatin/HA-Tyr Film. The VEGF (50 μL, [100 μg mL^{-1}]) and IL-4 (50 μL, [10 μg mL^{-1}]) solutions, both prepared in MilliQ water, were incubated for 12 h at 4 °C on top of each film. Then, the films were put in contact with PBS for release experiments or were kept dry in a sterile environment for cell culture experiments (2D or 3D).

DOI: 10.1021/acsomega.6b00502
ACS Omega 2017, 2, 918−929

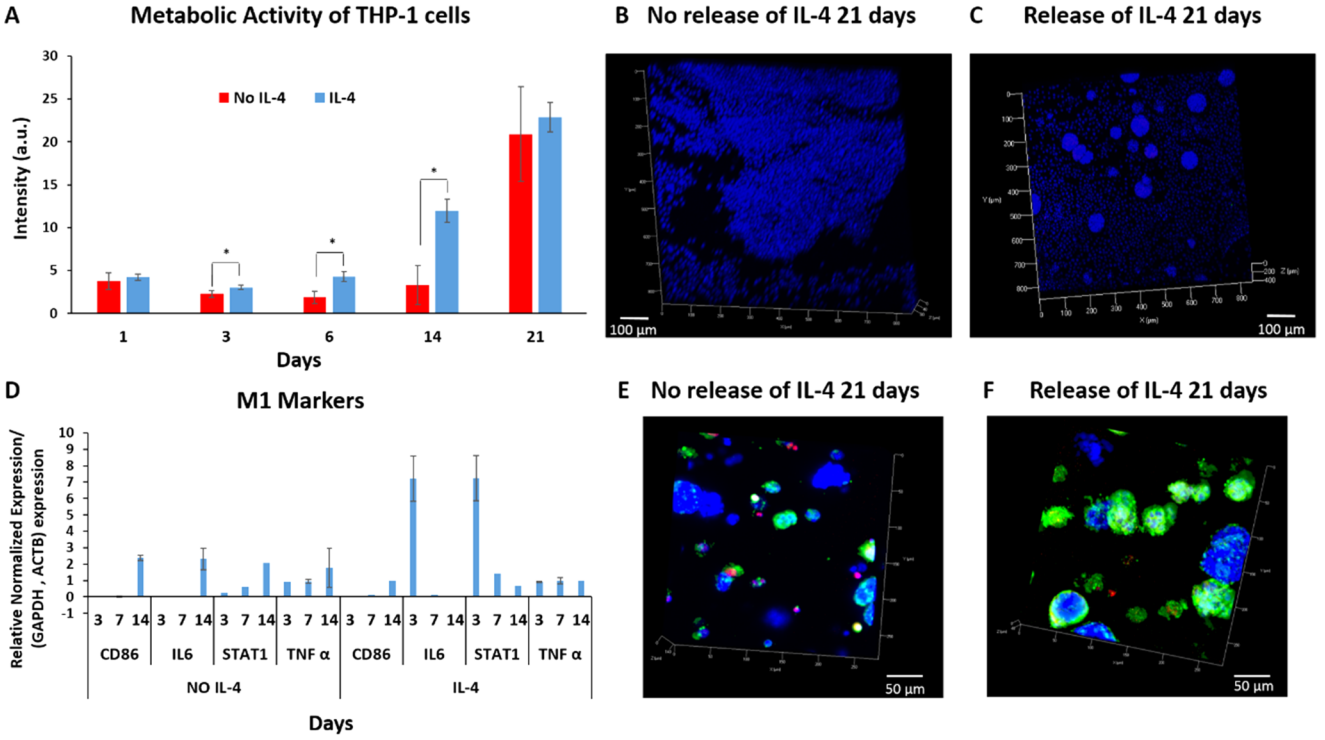

Figure 8. Release of IL-4 initially loaded in the gelatin/HA-tyr film to the hydrogel with THP-1 encapsulated in the hydrogel. (A) Metabolic activity of encapsulated THP-1 in gelatin hydrogel with and without IL-4 release from the film. (B, C) Confocal images of THP-1 encapsulated in the hydrogel by DAPI (blue) staining after 21 days with and without IL-4 release. (D) Results of real-time PCR analysis of M1 markers for 3D encapsulated THP-1 cells without or with IL-4 release. The M1 markers are as follows: CD86, IL-6, STAT1, and TNF-α. (E, F) Confocal images of THP-1 encapsulated in the hydrogel with the M1 marker, CD80 (red), and the M2 marker, CD206 (green) and DAPI (blue).

Release Kinetics of VEGF and IL-4 from the Films and Quantification of Cytokines in the Supernatant. For the release experiment of both VEGF and IL-4, the fresh buffer solution (1 mL) was added after each record and then supernatants were kept at −80 °C prior to analysis. The levels of cytokines were measured with ELISA Development Kits (VEGF, IL-4, IL1-RA, IL-6, IL-8, TNF-α, CCL18, PeproTech). Standard curves were constructed with the included standard protein in phosphate buffer. Samples were analyzed according to the manufacturer's protocol. The absorbance was measured at 450 nm with SpectraMax Paradigm.

Measurements of Elastic Modulus by AFM Nanoindentation. AFM experiments were carried out using a MFP3D-BIO instrument (Asylum Research Technology, Atomic Force F & E GmbH, Germany). The nanoindentation method provides Young's modulus calculated from the force versus indentation curve. Triangular cantilevers with colloidal probes (borosilicate glass sphere with a radius of 5 μm) were purchased from Novascan (Novascan Technologies, Inc., Iowa State University Research Park, IA). The spring constants of the cantilevers measured using a thermal noise method were found to be 60 pN nm^{-1}. Experiments were performed in PBS buffer (pH = 7.4) at room temperature. Elasticity maps and the corresponding histograms (statistic distribution) were estimated from the analysis of the approach curves according to the Dimitradis model[23]

$$F = \frac{4E}{3(1-\nu^2)} R^{1/2}\delta^{3/2}[1 + 1.133\chi + 1.283\chi^2 + 0.769\chi^3 - 0.0975\chi^4]$$

where δ is the indentation depth, ν is the Poisson coefficient, R is the colloid radius, and h is the sample thickness. The Dimitriadis correction for finite thickness is defined by the χ parameter

$$\chi = \frac{\sqrt{R\delta}}{h}$$

All of the force volume images were analyzed by means of an automatic Matlab algorithm described elsewhere.[24]

Cell Culture Experiments. *Two-Dimensional Cell Experiments (Culture on Top of the Film).* For cell experiments in 2D (cells seeded on top of the film), the studies were performed with HUVECs (Promocell) and THP-1 cells (human monocytic cell line; ATCC).

The HUVEC cells were used at passages between 4 and 8. The culture media used were endothelial cell growth medium (Promocell) supplemented with Supplement Mix C-39215. Cells, in a 75 cm^2 flask, were first cultivated to a near-confluent state and then they were trypsinized and counted prior to experiment. The THP-1 cells were cultured in RPMI 1640 GlutaMAX (Gibco Life Technologies) supplemented with 10% fetal bovine serum, 1% penicillin/streptomycin, 0.2% fungizone, and 0.05 nM 2-mercaptoethanol.

Gelatin and gelatin/HA films were UV-treated for 15 min. For each cell experiment, 50 000 cells were deposited on top of the films, the system was first put at 37 °C for 15 min for adhesion, and after that the medium was added. The plate was then put into the incubator at 37 °C.

Three-Dimensional Cell Experiments/Hydrogel Preparation for Cell Encapsulation. For cell experiments in 3D (cells encapsulated in gelatin type-A hydrogels), the main work was

DOI: 10.1021/acsomega.6b00502
ACS Omega 2017, 2, 918−929

performed with HUVECs and THP-1 cells. Prior to encapsulation, the cells (HUVECs and THP-1) were prepared according to the protocol described before (cf. "Two-Dimensional Cell Experiments (Culture on Top of the Film)" section).

For cell encapsulation in the hydrogels, the gelatin type-A solution was prepared in the cell culture medium. All of the solutions, gelatin, and TGA were filtered prior to use (0.22 μm). The cells were then trypsinized and centrifuged to obtain cell pellets. Then, the gelatin type-A solution was added to obtain a cell density of 2×10^6 cells mL^{-1} of the solution and kept in water bath at slightly above 37 °C. Then, 10 μL of TGA solution was added on each cross-linked gelatin/HA-tyr film (loaded or not with either VEGF or IL-4). The gelatin solution (50 μL) with encapsulated cells (100 000 cells/hydrogel) was then deposited on top of each film and mixed with the TGA solution to obtain homogeneous cross-linking and the film/hydrogel composite was then put into the incubator at 37 °C for at least 15 min prior to adding the cell culture medium in each well.

Biological Analyses. To check the metabolic activity of the cells cultivated on gelatin or gelatin/HA films, an in vitro toxicology assay kit, for a resazurin-based test (Sigma-Aldrich), was used. The protocol was carried out as described in the kit. For all immunofluorescent stainings, the cells were first fixed with a 3.7% (v/v) solution of paraformaldehyde (PFA) in PBS.

Calcein (Life Technologies) staining was used as a viable cell marker. After 3 days of experiment, the films (gelatin and gelatin/HA) with HUVECs were rinsed two times with PBS. Then, a solution of calcein-AM (5 μL for 100 μL of medium) was prepared and 150 μL of this solution was incubated on each film for 30 min at 37 °C. Finally, the cells were fixed with PFA. The pictures of the cells labeled with calcein dye were taken using a confocal microscope and were analyzed using Image J software.[25]

The apoptotic/necrotic/healthy cells detection kit (Promokine) was used to quantify the apoptotic (green fluorescence for FITC-Annexin), necrotic (red fluorescence for ethidium homodimer III), and healthy (blue fluorescence for Hoechst) cells with a fluorescent microscope.

To quantify the NO level via the detection of nitrite in the supernatant in 3D cell experiments with HUVECs, nitric oxide assay kit PK 210737 from Promokine was used and the test was performed according to provider's instruction. After the experiments, the samples were kept at −80 °C prior to analysis.

For HUVECs, the cells were then incubated in a Triton X-solution (0.1% in PBS) for 5 min. Then, two rinsing steps with PBS were performed and the samples were incubated for 20 min with the BSA solution (1% v/v) in PBS. DAPI/phalloidin/PECAM-1 (CD31) immunofluorescent stainings were performed. After fixation with PFA and incubation with Triton and BSA solution, the samples were incubated for 90 min with primary antibody PECAM-1 (CD31) (Mab mouse anti-human [0.938 mg mL^{-1}]; Thermo Scientific) at a dilution of 1/150 in PBS. Then, the samples were incubated for 30 min with secondary antibody (Goat anti-mouse IgG, Oregon green 488 conjugate [2 mg mL^{-1}]; Thermo Scientific) at a dilution of 1/200 in PBS and two rinsing steps with PBS were performed. After that, the samples were incubated for 1 h with phalloidin (Alexa Fluor 568 phalloidin [6.6 μM]; Molecular Probes Life Technologies) at a dilution of 1/40 in the BSA solution (1% v/v in PBS) and two rinsing steps in PBS were performed.

For THP-1, after fixation with PFA, the cells were washed twice with the Tween 20 solution (0.2% in PBS) for 5 min. The samples were incubated for 30 min with the BSA (3% v/v) and glycine (1%) solution in PBS. Then, two rising steps with 5% goat serum in PBS for 5 min each were performed. The samples were incubated with diluted primary antibodies and incubated at room temperature for 1 h. The primary antibodies were (i) mouse anti-human CD80 primary Ab (Thermo scientific) at a dilution of 1/200 in 5% (v/v) goat serum in PBS and (ii) rabbit anti-human CD206 primary Ab (Abcam) at a dilution of 1/176 in 5% (v/v) goat serum in PBS (final concentration = 1 μg mL^{-1}). The samples were rinsed 3 times with 0.2% Tween 20 for 5 min. The diluted secondary antibodies were incubated at room temperature for 1 h in the dark. The secondary antibodies were (i) Alexa Fluor-568 goat anti-mouse IgG (H + L) (Thermo scientific) for mouse anti-CD80 primary antibody at a dilution of 1/250 in 5% (v/v) goat serum in PBS (final concentration = 8 μg mL^{-1}) and (ii) Alexa Fluor-488 goat anti-rabbit IgG (H + L) (Thermo scientific) for Rabbit anti-CD206 primary antibody, 2 drops mL^{-1} of solution (in 5% v/v goat serum in PBS). The samples were rinsed three times with 0.2% Tween 20 for 5 min each time. Finally, the nuclei were labeled with DAPI (1 mg mL^{-1}; Promokine) at a dilution of 1/100 in PBS and two rinsing steps were performed.

Real-time reverse transcription qPCR (real-time RT-qPCR) was used for quantifying biologically relevant changes in the mRNA levels of THP-1-encapsulated cells. The expression levels of CD86, TNF, STAT1, CD163L1, IL10, and IL1RA were measured by real-time qPCR using 96-well Prime PCR custom plates (BIORAD). Reactions were carried out for 50 cycles in a CFX-Connect (BIORAD). GAPDH was used as a reference gene for all of the RT-qPCR obtained results.

■ ASSOCIATED CONTENT

Supporting Information

The Supporting Information is available free of charge on the ACS Publications website at DOI: 10.1021/acsomega.6b00502.

Additional information regarding film characterization and cytokine quantification (PDF)

■ AUTHOR INFORMATION

Corresponding Authors

*E-mail: philippe.lavalle@inserm.fr (P.L.).
*E-mail: e.vrana@protipmedical.com (N.E.V.).

ORCID

Helena Knopf-Marques: 0000-0002-6134-8129
Nihal Engin Vrana: 0000-0002-5398-6710

Author Contributions

$^{\nabla}$H.K.-M. and J.B. contributed equally.

Author Contributions

H.K.M., J.B., P.L., and N.E.V. designed the experiments. P.L. and N.E.V. supervised the experiments. H.K.M., J.B., B.V., G.K., H.S., and U.L. performed experiments. H.K.M., J.B., P.L., N.E.V., G.F., and J.B. analyzed and interpreted data. L.W. manufactured materials. H.K.M., J.B., and N.E.V. wrote the manuscript. All authors revised and corrected the final manuscript.

Notes

The authors declare no competing financial interest.

DOI: 10.1021/acsomega.6b00502
ACS Omega 2017, 2, 918−929

■ ACKNOWLEDGMENTS

This project has received funding from the European Union's Seventh Framework Programme for research, technological development and demonstration under grant agreement no. 602694 (IMMODGEL).

■ REFERENCES

(1) (a) Lee, K.; Silva, E. A.; Mooney, D. J. Growth factor delivery-based tissue engineering: general approaches and a review of recent developments. *J. R. Soc., Interface* **2011**, *8*, 153−170. (b) Franz, S.; Rammelt, S.; Scharnweber, D.; Simon, J. C. Immune responses to implants − A review of the implications for the design of immunomodulatory biomaterials. *Biomaterials* **2011**, *32*, 6692−6709.

(2) (a) Dumont, C. M.; Park, J.; Shea, L. D. Controlled release strategies for modulating immune responses to promote tissue regeneration. *J. Controlled Release* **2015**, *219*, 155−166. (b) Schultz, P.; Vautier, D.; Richert, L.; Jessel, N.; Haikel, Y.; Schaaf, P.; Voegel, J.-C.; Ogier, J.; Debry, C. Polyelectrolyte multilayers functionalized by a synthetic analogue of an anti-inflammatory peptide, α-MSH, for coating a tracheal prosthesis. *Biomaterials* **2005**, *26*, 2621−2630. (c) Lee, K. Y.; Mooney, D. J. Hydrogels for tissue engineering. *Chem. Rev.* **2001**, *101*, 1869−1880.

(3) Barthes, J.; Özçelik, H.; Hindié, M.; Ndreu-Halili, A.; Hasan, A.; Vrana, N. E. Cell microenvironment engineering and monitoring for tissue engineering and regenerative medicine: the recent advances. *BioMed Res. Int.* **2014**, *2014*, No. 921905.

(4) (a) Zhao, W.; McCallum, S. A.; Xiao, Z.; Zhang, F.; Linhardt, R. J. Binding affinities of vascular endothelial growth factor (VEGF) for heparin-derived oligosaccharides. *Biosci. Rep.* **2012**, *32*, 71−81. (b) Jackson, D. G. The lymphatics revisited - New perspectives from the hyaluronan receptor LYVE-1. *Trends Cardiovasc. Med.* **2003**, *13*, 1−7. (c) Kreuger, J.; Spillmann, D.; Li, J.-P.; Lindahl, U. Interactions between heparan sulfate and proteins: the concept of specificity. *J. Cell Biol.* **2006**, *174*, 323−327. (d) Zhu, Y.; Oganesian, A.; Keene, D. R.; Sandell, L. J. Type IIA Procollagen Containing the Cysteine-rich Amino Propeptide Is Deposited in the Extracellular Matrix of Prechondrogenic Tissue and Binds to TGF-β1 and BMP-2. *J. Cell Biol.* **1999**, *144*, 1069−1080.

(5) Chaubaroux, C.; Perrin-Schmitt, F.; Senger, B.; Vidal, L.; Voegel, J.-C.; Schaaf, P.; Haikel, Y.; Boulmedais, F.; Lavalle, P.; Hemmerlé, J. Cell Alignment Driven by Mechanically Induced Collagen Fiber Alignment in Collagen/Alginate Coatings. *Tissue Eng., Part C* **2015**, *21*, 881−888.

(6) Barthes, J.; Vrana, N. E.; Özçelik, H.; Gahoual, R.; François, Y. N.; Bacharouche, J.; Francius, G.; Hemmerlé, J.; Metz-Boutigue, M.-H.; Schaaf, P. Priming cells for their final destination: microenvironment controlled cell culture by a modular ECM-mimicking feeder film. *Biomater. Sci.* **2015**, *3*, 1302−1311.

(7) Xu, X.; Jha, A. K.; Harrington, D. A.; Farach-Carson, M. C.; Jia, X. Hyaluronic acid-based hydrogels: from a natural polysaccharide to complex networks. *Soft Matter* **2012**, *8*, 3280−3294.

(8) (a) Collins, M. N.; Birkinshaw, C. Hyaluronic acid based scaffolds for tissue engineering—A review. *Carbohydr. Polym.* **2013**, *92*, 1262−1279. (b) Vercruysse, K. P.; Marecak, D. M.; Marecek, J. F.; Prestwich, G. D. Synthesis and in vitro degradation of new polyvalent hydrazide cross-linked hydrogels of hyaluronic acid. *Bioconjugate Chem.* **1997**, *8*, 686−694. (c) Bencherif, S. A.; Srinivasan, A.; Horkay, F.; Hollinger, J. O.; Matyjaszewski, K.; Washburn, N. R. Influence of the degree of methacrylation on hyaluronic acid hydrogels properties. *Biomaterials* **2008**, *29*, 1739−1749. (d) Camci-Unal, G.; Cuttica, D.; Annabi, N.; Demarchi, D.; Khademhosseini, A. Synthesis and characterization of hybrid hyaluronic acid-gelatin hydrogels. *Biomacromolecules* **2013**, *14*, 1085−1092. (e) Chen, J. P.; Leu, Y. L.; Fang, C. L.; Chen, C. H.; Fang, J. Y. Thermosensitive hydrogels composed of hyaluronic acid and gelatin as carriers for the intravesical administration of cisplatin. *J. Pharm. Sci.* **2011**, *100*, 655−666. (f) Knopf-Marques, H.; Pravda, M.; Wolfova, L.; Velebny, V.; Schaaf, P.; Vrana, N. E.; Lavalle, P. Hyaluronic Acid and Its Derivatives in Coating and Delivery Systems: Applications in Tissue Engineering, Regenerative Medicine and Immunomodulation. *Adv. Healthcare Mater.* **2016**, *5*, 2841.

(9) (a) Dong, Z.; Wang, Q.; Du, Y. Alginate/gelatin blend films and their properties for drug controlled release. *J. Membr. Sci.* **2006**, *280*, 37−44. (b) Draye, J.-P.; Delaey, B.; Van de Voorde, A.; Van Den Bulcke, A.; Bogdanov, B.; Schacht, E. In vitro release characteristics of bioactive molecules from dextran dialdehyde cross-linked gelatin hydrogel films. *Biomaterials* **1998**, *19*, 99−107. (c) Yamamoto, M.; Ikada, Y.; Tabata, Y. Controlled release of growth factors based on biodegradation of gelatin hydrogel. *J. Biomater. Sci., Polym. Ed.* **2001**, *12*, 77−88. (d) Young, S.; Wong, M.; Tabata, Y.; Mikos, A. G. Gelatin as a delivery vehicle for the controlled release of bioactive molecules. *J. Controlled Release* **2005**, *109*, 256−274.

(10) (a) Zhang, J.; Senger, B.; Vautier, D.; Picart, C.; Schaaf, P.; Voegel, J.-C.; Lavalle, P. Natural polyelectrolyte films based on layer-by layer deposition of collagen and hyaluronic acid. *Biomaterials* **2005**, *26*, 3353−3361. (b) Highberger, J. H.; Gross, J.; Schmitt, F. O. The interaction of mucoprotein with soluble collagen; an electron microscope study. *Proc. Natl. Acad. Sci. U.S.A.* **1951**, *37*, 286−91.

(11) Jin, R.; Lou, B.; Lin, C. Tyrosinase-mediated in situ forming hydrogels from biodegradable chondroitin sulfate-tyramine conjugates. *Polym. Int.* **2013**, *62*, 353−361.

(12) Santoro, M.; Tatara, A. M.; Mikos, A. G. Gelatin carriers for drug and cell delivery in tissue engineering. *J. Controlled Release* **2014**, *190*, 210−218.

(13) Hosack, L. W.; Firpo, M. A.; Scott, J. A.; Prestwich, G. D.; Peattie, R. A. Microvascular maturity elicited in tissue treated with cytokine-loaded hyaluronan-based hydrogels. *Biomaterials* **2008**, *29*, 2336−2347.

(14) Sinha, V. R.; Singla, A. K.; Wadhawan, S.; Kaushik, R.; Kumria, R.; Bansal, K.; Dhawan, S. Chitosan microspheres as a potential carrier for drugs. *Int. J. Pharm.* **2004**, *274*, 1−33.

(15) Wang, Y.; Kim, H.-J.; Vunjak-Novakovic, G.; Kaplan, D. L. Stem cell-based tissue engineering with silk biomaterials. *Biomaterials* **2006**, *27*, 6064−6082.

(16) Lee, S. H.; Lee, Y.; Chun, Y. W.; Crowder, S. W.; Young, P. P.; Park, K. D.; Sung, H. J. In Situ Crosslinkable Gelatin Hydrogels for Vasculogenic Induction and Delivery of Mesenchymal Stem Cells. *Adv. Funct. Mater.* **2014**, *24*, 6771−6781.

(17) Huang, Y.; Luo, Q.; Zha, G.; Zhang, J.; Li, X.; Zhao, S.; Li, X. Biomimetic ECM coatings for controlled release of rhBMP-2: construction and biological evaluation. *Biomater. Sci.* **2014**, *2*, 980−989.

(18) Crouzier, T.; Ren, K.; Nicolas, C.; Roy, C.; Picart, C. Layer-By-Layer Films as a Biomimetic Reservoir for rhBMP-2 Delivery: Controlled Differentiation of Myoblasts to Osteoblasts. *Small* **2009**, *5*, 598−608.

(19) Barthes, J.; Mertz, D.; Bach, C.; Metz-Boutigue, M.-H.; Senger, B.; Voegel, J.-C.; Schaaf, P.; Lavalle, P. Stretch-induced biodegradation of polyelectrolyte multilayer films for drug release. *Langmuir* **2012**, *28*, 13550−13554.

(20) Patel, Z. S.; Yamamoto, M.; Ueda, H.; Tabata, Y.; Mikos, A. G. Biodegradable gelatin microparticles as delivery systems for the controlled release of bone morphogenetic protein-2. *Acta Biomater.* **2008**, *4*, 1126−1138.

(21) Li, A.; Dubey, S.; Varney, M. L.; Dave, B. J.; Singh, R. K. IL-8 directly enhanced endothelial cell survival, proliferation, and matrix metalloproteinases production and regulated angiogenesis. *J. Immunol.* **2003**, *170*, 3369−3376.

(22) Tsuchiya, S.; Kobayashi, Y.; Goto, Y.; Okumura, H.; Nakae, S.; Konno, T.; Tada, K. Induction of maturation in cultured human monocytic leukemia cells by a phorbol diester. *Cancer Res.* **1982**, *42*, 1530−1536.

(23) Dimitriadis, E. K.; Horkay, F.; Maresca, J.; Kachar, B.; Chadwick, R. S. Determination of elastic moduli of thin layers of soft material using the atomic force microscope. *Biophys. J.* **2002**, *82*, 2798−2810.

DOI: 10.1021/acsomega.6b00502
ACS Omega 2017, 2, 918−929

(24) Polyakov, P.; Soussen, C.; Duan, J.; Duval, J. F.; Brie, D.; Francius, G. Automated force volume image processing for biological samples. *PLoS One* **2011**, *6*, No. e18887.
(25) Rasband, W. S. *ImageJ, U.S.*; National Institutes of Health: Bethesda, Maryland, 1997−2011.

DOI: 10.1021/acsomega.6b00502
ACS Omega 2017, 2, 918−929